NUMERICAL SIMULATION OF AIR JET ATTACHMENT TO CONVEX WALLS AND APPLICATIONS

Nikola Mirkov*, Bosko Rasuo**
***PhD student, Institute of Nucelar Sciences "Vinča", Laboratory for Thermal Engineering and Energy, **University of Belgrade, Faculty of Mechanical Engineering**

Keywords: *Coanda-Effect, Unmanned Air Vehicles, Computational Fluid Dynamics*

Abstract

The air jets have a natural tendency do attach to walls when blown close to them. After the air jet is issued into the quiescent surrounding it entrains the air between the jet and the wall. Low pressure region is formed causing the jet to deflect towards the wall. This phenomenon known by the name of the Coanda-effect had found diverse applications ever since it was discovered. Many disc shaped vertical take-off and landing (VTOL) aircraft designs use Coanda-effect to generate the vertical thrust to lift the aircraft. Several design issues of such aircraft are investigated in this paper using computational fluid dynamics approach.

1 Introduction

Owing to the unmanned air vehicles (UAV's), interest for the aircraft, that produce lift with the aid of the Coanda-effect, renewed in recent times. There is a considerable base of proponents of Coanda-effect UAV's on the internet, new web-sites addressing the topic appearing frequently. The need to address these topics in a systematic way is present.

This paper is concerned with numerical investigation of several possible configurations. Although UAV's are relatively easy to build and test we believe that numerical simulation still brings some advantages, as well as time and effort savings.

It is assumed that the lift such UAV produce, rises with the surface to which the jet attaches. The attached jet produces more lift. So, it is our intention to have the wall jet attached to the surface as further as possible. It is intuitively clear that more curved surface will cause the jet to detach from the surface sooner, in other words, large curvature promotes detachment. Therefore, there is a need to test several configurations with increasing the curvature of the lifting surface.

The sketch of Coanda-effect UAV is given in Fig.1. It represents an artistic impression of a Jean-Louis Naudin's [5] UAV test flight.

Fig. 1. The artistic impression of a Coanda-effect UAV at flight.

Configurations that have been tested during this study are produced by varying entries in class function, shape function representation of geometry, which will be described in the following section. The axial symmetry of the flow is one assumption when 2D simulations are carried out.

It is known that injecting the fluid "energizes" the boundary layer making it less prone to premature separation. Few solutions of this sort will also be numerically tested.

There are several battery-powered prototypes of UAV's that demonstrated lift generation and control using Coanda-effect.

Among the examples is UK-based Geoff's Flying Saucer (GFS) Projects [7]. It demonstrated the Coanda-effect unmanned air vehicle having 0.91m diameter, and weight of 5.45kg. Other attempts [5] also had similar size aircraft, therefore the diameter of 1m is adopted for this study.

The flight test carried so far by Geoff Haton [7] and Jean-Louis Naudin [5] revealed that battery-powered vertical take-off and landing vehicles have small endurance. That brings to conclusion that the power available for the hover and maneuvering should be used as economically as possible. A need for thorough experimental and numerical test is obvious. The present study aims at contributing to those efforts with several new ideas.

2 Definition of Geometry

The way geometry is represented strongly affects the optimization process.

In the recent paper by Kuflan [3], it is shown how different airfoils, axially symmetric bodies, and other more complex three dimensional shapes (wings, fuselages, etc.) can be represented by means of class function, shape function representation.

The class function is used to define general class of geometries, while shape function is used to define specific shapes within the geometry class.

The main idea presented in [3] is to decompose the basic shape into scalable elements corresponding to discrete components, by representing the shape function with a Bernstein polynomial. The Bernstein polynomial of order n is composed of the $n+1$ terms of the form:

$$S_{r,n}(\psi) = K_{r,n}\psi^{r}(1-\psi)^{n-r} \qquad (1)$$

$$K_{r,n} \equiv \binom{n}{r} \equiv \frac{n!}{r!(n-r)!} \qquad (2)$$

Where factors $K_{r,n}$ are binomial coefficients as shown above. Fig. 2 shows an example of unit function decomposition using Bernstein polynomials of sixth degree. By scaling any component in the unit function representation we can make well localized, small variations of that function.

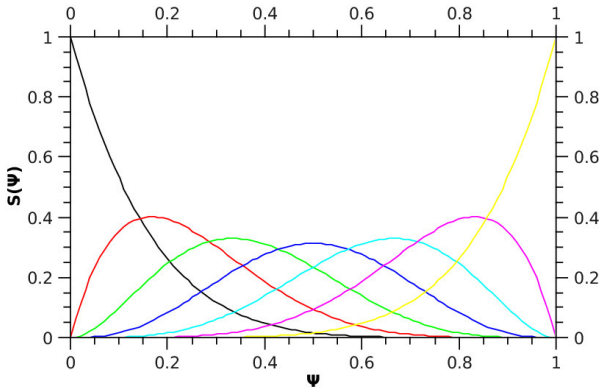

Fig. 2. The unit function decomposition using Bernstein polynomials

Usually geometry of cross section of typical Coanda-effect UAV is "elliptic-arc-like". Therefore the class function will be the function defining an elliptic arc.

$$\varsigma(\psi) = A \cdot \psi^{0.5}(1-\psi)^{0.5} \qquad (3)$$

By adjusting the coefficient A in the class function representation one can choose the aspect ratio of an elliptic arc. Taking A to be equal to two, gives a circle. By scaling the coefficients in the component representation of a shape function, we can derive appropriate variations of the basic shape. Fig. 3. shows decomposition of an ellipse (A=0.7) using Bernstein polynomials of sixth degree. We need to stress that the order of Bernstein polynomial, used for the function decomposition, is chosen freely. The higher order renders more localized variations of the basic shape possible.

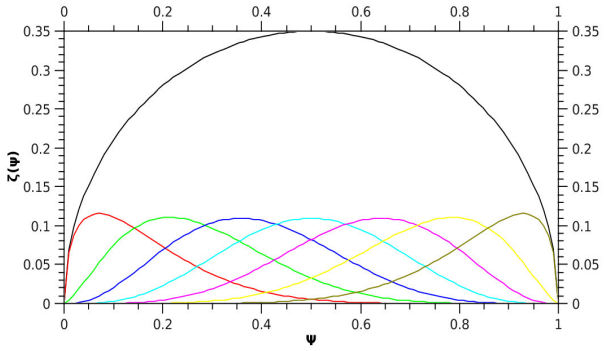

Fig. 3. Decomposition of an ellipse using Bernstein polynomials

For our simulation we used geometry defined by following expressions. The upper contour is defined by

$$C_u(\psi) = \varsigma(\psi) \cdot S(\psi) \tag{4}$$

where

$$\varsigma(\psi) = 0.7 \cdot \psi^{0.5}(1-\psi)^{0.5} \tag{5}$$

and

$$S(\psi) = 1 \tag{6}$$

with

$$\psi \in [0.5,1] \tag{7}$$

The lower contour is defined by

$$C_l(\psi) = -0.25 \cdot C_u(\psi) \tag{8}$$

Using this method we define various contour shapes by scaling components of Bernstein polynomial representation of the unit shape function. This technique has following properties [3]:

- This contour representation technique captures the entire design space of smooth geometries.
- Every contour in the entire design space can be derived from the unit shape function contour.
- Every contour in the design space is derivable from every other.

With this technique it will be easy to construct various shapes of the UAV based on Coanda-effect and compare their performances.

3 Means of flow optimization

It is widely recognized that not only good aerodynamic shape is important for overall aerodynamics performance. Rather than just choosing the right geometry which will enable required flow picture one can also employ active measures of flow control such as blowing the air into, or sucking the air out of the air jet layer adjacent to the wall.

Actually, these measures are the most frequent applications of the Coanda-effect in aeronautics. The Coanda-effect is often employed for increasing the lift for Short Take Off and Landing (STOL) aircraft, i.e. by blowing air jet down the wing flaps.

4 Numerical Solution

The geometry of the lifting body considered in this study is axially symmetric allowing simulated domain to be two-dimensional. Fig. 4 shows the flow domain decomposed using structured numerical mesh. The mesh consists of 24000 cells which are refined towards the wall.

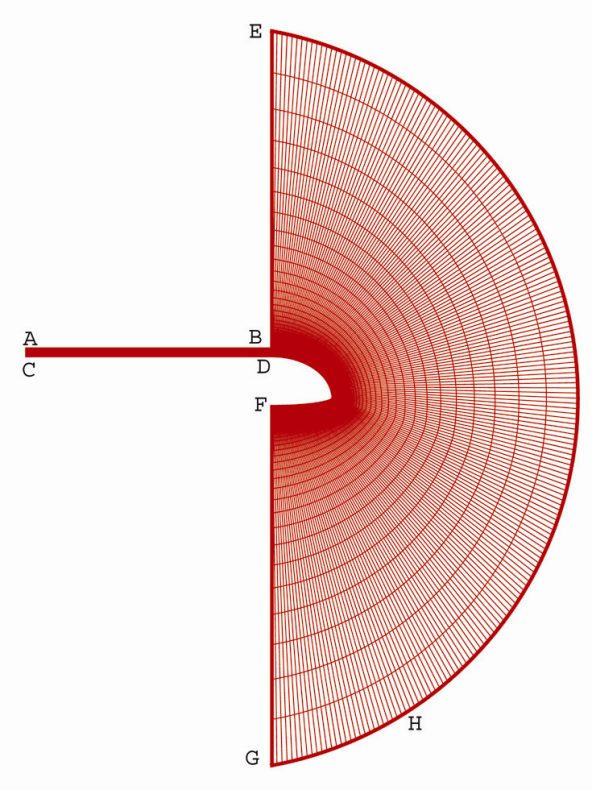

Fig.4. Numerical mesh

The rectangular domain ABCD visible on Fig. 4 represents a channel, having length to height ratio equal to 20. Instead of simply prescribing turbulent inflow, this channel is used as a sort of precursor domain, as it is estimated that this ratio will be enough for fully developed turbulence to emerge at the slot where air jet enters the domain of interest. Also, on the Fig. 4. are line of symmetry EG, circular arc EHG representing the outflow boundary, and curve DF representing the body where attachment of the air jet due to Coanda-effect takes place. The air inlet BD is 0.05 m wide. The diameter of the aircraft is taken to be 1 m.

The velocity magnitude at the inflow boundary is taken to be 20 m/s. This was back-of-the-envelope estimate, not a result of a measurement. It may differ from the value found at the actual aircraft. Naudin [5] provides the results of some experiments of Coanda-effect based trust. The value we used for our study is found in the middle of the velocity magnitude range in that study. It will be interesting, and it is planned for the future study, to see how varying inflow velocity effects lift, and to what point lift is found to increase with inflow velocity. Also, the same is true for the conditions at the inflow/outflow slot where the measures of active flow control are applied.

Reynolds averaged Navier-Stokes (RANS) equations with two-equation $k-\omega$ Shear Stress Transport (SST) model [2] serving as a turbulence closure, are solved using ANSYS Fluent code [4]. RANS equations and the SST model will not be reproduced here since they can easily be found in the literature [1]. The SST model merges $k-\varepsilon$ and $k-\omega$ and seeks to combine the positive features of both models. Since $k-\omega$ needs no dumping function, it is employed in a sublayer of a boundary layer. Also it is employed in logarithmic region, whereas $k-\varepsilon$ is employed in the wake region and free shear layer. These attributes made it quite popular for the aerodynamic applications.

The simulations we carried out are two-dimensional, steady state. The pressure correction and momentum equations are solved iteratively using SIMPLE algorithm. The discretization schemes are second-order.

4 Results

What we are aspiring is reaching the best overall aerodynamic performance for the specific UAV. Probably, the most important output value resulting either from experiment on these UAV's or by the numerical simulation is inlet velocity to thrust ratio for a given inlet size and dimension of the lifting body.

The Fig. 5 shows contours of pressure and the streamline pattern in the front for the basic case, that is the one without active flow control.

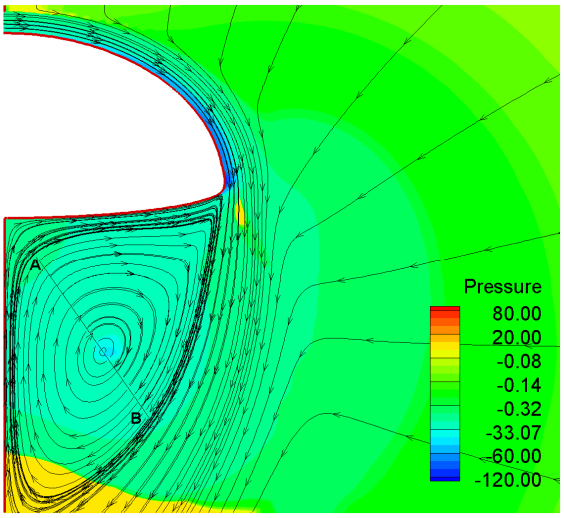

Fig. 5. The streamlines and pressure contours [Pa]. The basic case.

The line AB on Fig. 5 is streamline termination line and is here just for auxiliary purpose. The vertical force this body created under described flow conditions was 13.79 *N*. The creation of a vortex below the aircraft is visible. For the axially symmetric body this becomes a ring vortex and lift characteristics are related to it. The rotation of a vortex ring propels the body upwards.

In the Fig. 6. same is shown for the case of active flow control by suction. The suction is enforced by pressure difference at the slot located at the body contour (point C). The pressure difference was 10 *kPa.* Here we see that diameter of the vortex ring decreased. The total force in vertical direction was 15.68 *N*.

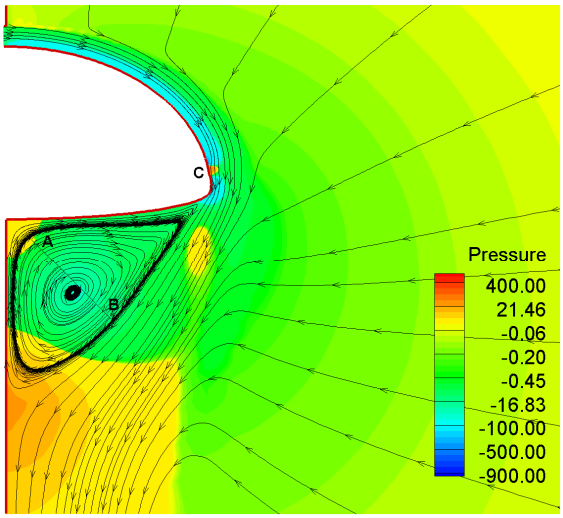

Fig. 6. The streamlines and pressure contours [Pa]. The flow control by suction.

The Fig. 7. shows distribution of the pressure coefficient along the contour for the case of active flow control by sucking.

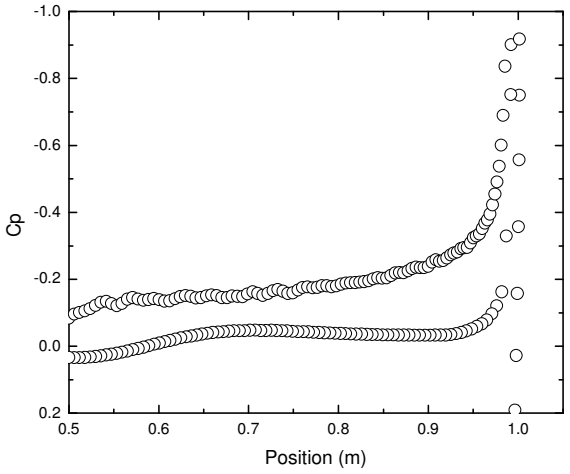

Fig. 7. The coefficient of pressure - flow control by suction

In the case of blowing, the jet opening is in the same position on the contour as for suction (point C in Fig. 6.). The air jet is blow tangentially to the surface with velocity *10 m/s*. Blowing the jet has different effect on flow picture than previous case. The Fig. 8. displays streamlines and contours of pressure for this case. More surrounding air has been entrained and forced downwards. This didn't lead to increase in vertical thrust.

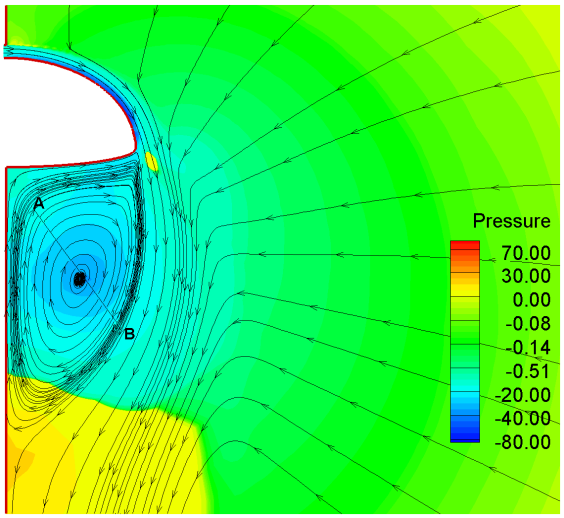

Fig. 8. The streamlines and pressure contours [Pa]. The flow control by blowing high pressure air.

The total force in vertical direction was 13.37 *N*. The Fig. 9. shows distribution of the pressure coefficient along the contour for the case of active flow control by blowing.

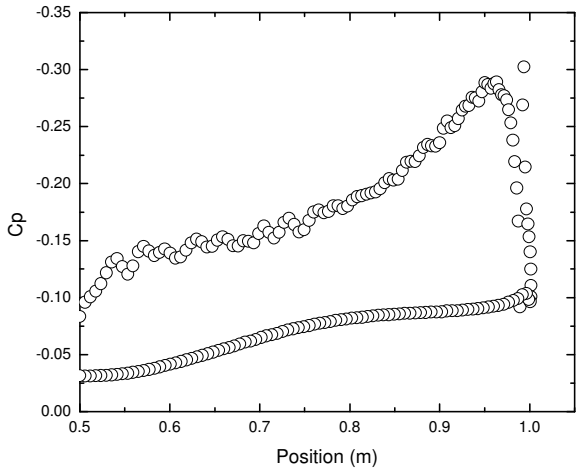

Fig. 9. The coefficient of Pressure - flow control by blowing.

Finally, we show the case inspired by "Astro kinetics-Dynafan" design (1964) [6]. The jet is blown very close to the edge believing that this will cause better results because of the short air jet attachment length. The jet doesn't lose energy due to friction with the wall as in the above cases (Fig. 10). Unfortunately, we couldn't confirm that hypothesis in our simulations. The reason is, because of the

Coanda-effect, this jet is able to stay attached almost to the end of the bottom wall, disabling the creation of the vortex ring below and the total lifting force acting on an aircraft was negative.

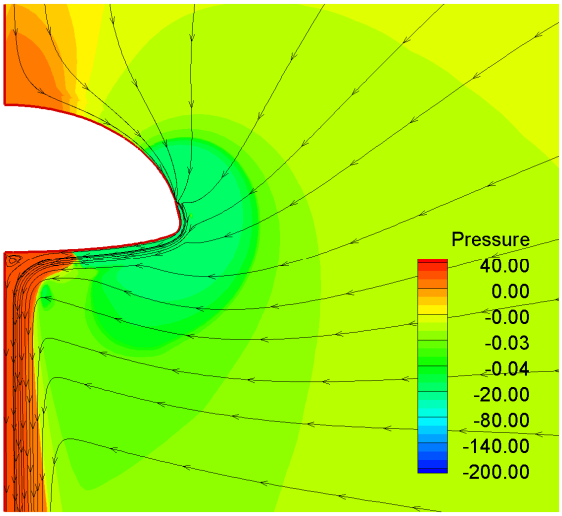

Fig. 10. The streamlines and the pressure contours [*Pa*] for a flow configuration inspired by Astro Kinetics-Dynafan design.

5 Conclusions

In this paper, we tested numerically several configurations of UAV's using Coanda-effect for thrust generation. The configurations were simulated with and without active flow control by suction and blowing from the slot located at the aircraft's body.

It is shown how mathematically define geometry design space of these aircraft in a manner similar to the one employed in the aircraft industry with solving optimization problems in mind.

The results included streamline patterns, the pressure contours and distribution of the pressure coefficient along the contours. The explanation for better performance of cases with active flow control may be prescribed to enhancing the circulation of a vortex ring situated below the aircraft. By suction we enable the wall jet to follow the contour longer before the detachment which results in a decrease in diameter of a vortex ring. This in turn causes stronger circulation, entrainment of surrounding air, and a pressure force on the lower part of the body causing the body to propel upwards.

A few things still need to be in place for this study to be complete. The optimization procedure, which would use numerical results as an input and available geometry definition using the class function, shape function approach. The detailed experiments measuring lift force for several geometries, under various flow conditions that are needed to validate previous numerical results are planed.

We conclude this paper with an observation we strongly believe is true. It is clear that Coanda-effect represents very interesting aerodynamic phenomenon, which still has to be fully exploited by aeronautical science.

References

[1] Blazek J. *Computational Fluid Dynamics: Principles and Applications*. 1st edition, Elsevier, 2001.

[2] Menter, F. R. Two-Equation Eddy-Viscosity Turbulence Models for Engineering Applications *AIAA Journal*, Vol. 32, No. 8, pp 1598-1605, August 1994.

[3] Kulfan B. M. Universal Parametric Geometry Representation Method *Journal of Aircraft*, Vol. 45, No. 1, pp 142-158, 2008.

[4] ANSYS Fluent 12.1 – User's guide.

[5] http://www.jlnlabs.org

[6] http://www.laesieworks.com/ifo/lib/VTOLdiscs.html

[7] http://en.wikipedia.org/wiki/GFS_Projects

Acknowledgement

The authors wish to express gratitude for the financial support of their research by Serbian Ministry of Science, through projects No. TR-18004 and TR-18033 respectively.

Contact Author Email Address

nmirkov@vinca.rs; brasuo@mas.bg.ac.rs

Copyright Statement